Indonesian Geotechnical Journal, April 2022, Vol 1 (1). Page 1-14
DOI: https://doi.org/10.56144/igj.v1i1.4
E-ISSN 2829-7520
https://indonesian-geotechnical-journal.org/index.php/JGI/issue/archive

Parametric Study of Tunnel Analysis in Clay shale on Short-Term and Long-Term Conditions Using Finite Element Method

Danang Setiya Raharja[1*], I Wayan Sengara[2], Imam Achmad Sadisun[3]
[1]Department of Civil Engineering, Faculty of Civil and Environmental Engineering, Institute Technology Bandung, Bandung, Indonesia, 40132; raharjadanang@gmail.com
[2]Department of Civil Engineering, Faculty of Civil and Environmental Engineering, Institute Technology Bandung, Bandung, Indonesia, 40132; wayansengara@yahoo.com
[3]Department of Geological Engineering, Faculty of Earth Sciences and Technology, Institute Technology Bandung, Bandung, Indonesia, 40132; sadisun@gmail.com
*****Correspondence: raharjadanang@gmail.com

SUBMITTED 25 March 2022 **REVISED** 15 April 2022 **ACCEPTED** 17 April 2022

ABSTRACT This study aims to determine the characteristics and classification of clay shale in West Java and their implications for tunnel stability under short and long-term conditions using the finite element method. Data were collected from projects in West Java containing clay shale spread over four rock formations, namely Cihoe (Tpc), Subang (Tms), Cantayan (Mtts/Mttc), and Jatiluhur (Tmj). Each formation has varying mechanical and engineering properties. The value of SPT from Cihoe formation can be categorized in three conditions, SPT < 40, SPT 40-60, and SPT > 60 for fully, highly to moderately, and slightly weathered, respectively. Meanwhile, the value of SPT of Subang formation can be categorized in two conditions, SPT < 60 and SPT >60 for fully and highly weathered, respectively. The data collected were analyzed to determine the Mohr-Coulomb (MC) and Hardening Soil (HS) parameters for Plaxis modeling. The model applied three variations of overburden thickness between 3 times, 6 times, and 9 times the tunnel diameter (3d, 6d, and 9d respectively). The greater the overburden thickness, the lower the surface deformation. The HS model gives better results than the MC model because it considers non-linearity. The minimum effective parameters needed to support tunnel during construction to meet the allowable deformation for 3d overburden conditions and the particular reinforcement system are c' 53kPa, ϕ' 28°, and $E'_{50}{}^{ref}$ 30,000 kPa. Long-term conditions possess lower stability than short-term, while prolonged deformations increase after construction and provide a rise in tunnel lining stress that needs to be considered in the design stage. The application of 2D tunnel modeling needs to be carefully analyzed, thereby representing the behavior of a continuous or 3D tunnel structure.

KEYWORDS Clay shale; Finite element; Mohr-Coulomb; Hardening soil; Tunnel

1 INTRODUCTION

In the past few decades, the transportation sector has been significantly developed, resulting in higher operational speed on highways or railways. This requirement needs to be supported with horizontal and vertical alignment infrastructure. Unfortunately, Indonesia has many hilly areas, such as West Java, wherein the alignment follows the contour under normal circumstances. There are two essential solutions for constructing a straight road: flyovers between the hills or mountain tunnels. On the other hand, tunnel construction in West Java faces a new challenge, namely clay shale formation. Clay shale is layer of clay with high shear strength during the dry condition but will easily destroyed when exposed to water and air (Zarkasi et al., 2018). Moreover, from an engineering point of view, shale is an essential material because it constitutes approximately 50% of the rock either exposed on the earth's surface or buried under a thin layer of sediment. All rocks in this category consist of clay or silt deposits that possess their present characteristics due to relatively moderate pressure and temperature (Terzaghi, Peck, & Mesri, 1996). Clay shales are usually the outcome of deposition and subsequent physical, chemical, or tectonic processes associated with the formation of outcrops along the Apennines. These sediments were deposited over 10 million years ago in the marine environment due to turbulent flows at the base of the continental crust. Its main characteristics depend on the

shape of the basin, receding period, and layering (Bonini et al., 2009). Meanwhile, from the geological, geotechnical, and environmental sciences' perspective, clay shale is one of the most complex materials. It exhibits a special behavior in that it tends to change rapidly from rock to soil and is generally considered a problematic material. In most cases, clay shale formations are influenced by the type of constituent minerals and changes in climate, physiography, and topography of the area being investigated (Deen, 1981).

Previous research has been constructed in clay shale layers in Opalinus, Switzerland, simulated using the Abaqus 3-dimensional (3D) finite element method under short and long-term conditions. The stresses built around tunnel lining are highly dependent on its material properties, excavation process, and speed. Unfortunately, the accumulation of negative excess pore pressure during the tunnel construction process boosts short-term stability. As a function of time, its dissipation reduces the effective stress on the soil and increases that in the tunnel structure (liner) (Bobet & Einstein, 2008).

Therefore, this study aims to determine the characteristics and classification of clay shale layers in West Java and review its implications on tunnel stability under short and long-term conditions using the finite element method.

2 MATERIAL AND METHODOLOGY

2.1 Data Collection and Characterization

Secondary data obtained from soil investigation projects carried out in West Java, as well as reports, journals, and references from preliminary studies, were utilized. However, not all collected data were subjected to completely laboratory tests, just a few were tested with the triaxial CU test, which was used to obtain soil parameters for modeling. The results of data characterization show that clay shale in West Java is spread out in the Cihoe Formation (Tpc), Subang Formation (Tms), Cantayan Formation (Mtts/Mttc), and Jatiluhur Formation (Tmj), as shown in Table 1. Characterization of clay shale in west java (Achdan & Sudana, 1992; Sudjatmiko, 1972; Effendi at al., 1998).

Table 1. Characterization of clay shale in west java

Criteria	Location of Sample						
	Deltamas Cikarang	HSR-Karawang	Slope DK52	Slope DK67	HSR-Walini	Walini Tunnel	Sentul
Geological Formation	(T_{pc}) Cihoe Formation	(Tms) Subang Formation	(Tms) Subang Formation	(Tms) Subang Formation	(Mtts) Cantayan Formation	(Mtts) Cantayan Formation	(Tmj) Jatiluhur Formation
N-SPT (clay shale)	20 - 40	24 - 100	>60	>60	39 - 100	>50	14 - 100
Depth of Clay shale Layer	9 m	20 m	6 m	6 m	10 - 25 m (oblique insert)	oblique insert	10 m
Activity (average)	1	0,75 - 3	0,75 - 1.5	0,5 - 0,75	0,75	-	-
Potential of Expansiveness	Very High	Very High	Very high	Low to medium	Very High	-	-
Relationship (PL - Wn - LL)	Plastic	Plastic to Solid	Plastic to Solid	Plastic	Plastic to Solid	Plastic	Plastic
Plasticity (LL – PL - PI)	High	High	High	Low	High	Low	High

The Cihoe Formation (Tpc) is categorized in the tertiary period of the Pliocene. It is characterized by a high plasticity, and the average activity value is 1. The potential for expansiveness is very high;

it was founded at a depth of ±10 m from the surface. The value of SPT can be categorized in three conditions, SPT < 40, SPT 40-60, and SPT > 60 for fully, highly to moderately, and slightly weathered, respectively.

The Subang Formation (Tms) is categorized in the Tertiary period during the late Miocene, and it has different characteristics from west to east. These include from high to low plasticity, the average activity value is approximately within 2 to 0.75, the potential for expansiveness is from very high to low, and it was founded at a depth of relatively ±20m to ±6m. The value of SPT is categorized in two conditions, SPT < 60 and SPT >60 for fully and highly weathered, respectively.

The Cantayan Formation (Mtts/Mttc) is in the Tertiary period during the late Miocene, has low to high plasticity characteristics, activity value of approximately 0.5 to 1, very high potential for expansiveness and the presence of layers forming an inclined plane. The Jatiluhur Formation (Tmj) is in the Tertiary period during the early Miocene, has high plasticity characteristics, and is found at a depth of ±10 m.

2.2 Soil Parameter Interpretation

Determination of soil parameters needs a reasonable interpretation due to its high variation, and not all samples have been thoroughly tested. Some were generalized by combining actual data and its correlation from references. This study assumes that clay shale is categorized as soil with a hard consistency. Based on some preliminary studies (Look, 2007; Bonini et al., 2009; Bowles, 1996; Ameratungga et al., 2016), the unit weight is between 18 to 20 kN/m^3. The permeability value is less than and equal to (≤) 10^{-7} m/s, the modulus of elasticity in the short and long terms is within 40 to 80 MPa and 30 to 60 MPa, respectively. The research on Opelinus clay shale soil, Italy, showed variations in its permeability ranging from 10^{-9} m/s to 10^{-12} m/s.

Effective shear strength parameters employed Gartung's (1986) suggestion as a reference to determine the weathering degree. These were divided into zones I (unweathered) to IV (final stage of weathering process) (Figure 1), with a slow triaxial test $\phi_r' = 8.6^0$ used to obtain the residual value. It was conservatively used for analysis, whereas the peak strength value makes the evaluation unsafe. For design purposes, Gartung suggested that the long-term parameters be reduced to $\phi'=20^0$ and c' = 20 kPa. This research adopted a statistical approach and fitting method to determine shear strength, modulus, and lateral earth pressure (K_0).

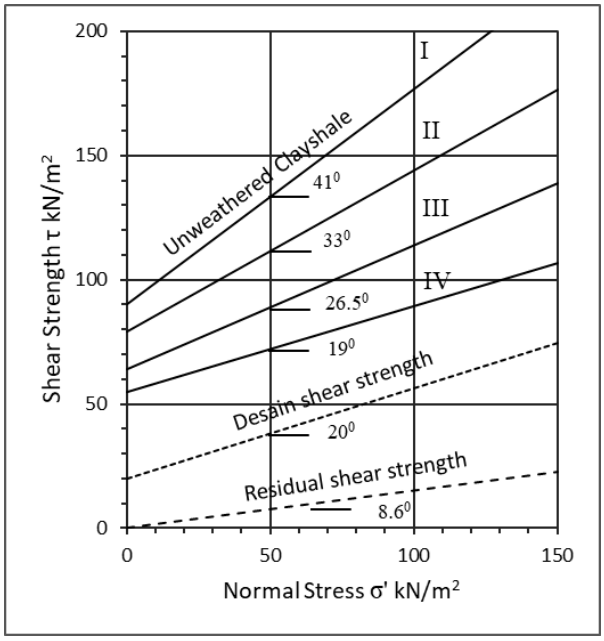

Figure 1. Effective shear strength parameters use the suggestion from Gartung (1986) (op cit. Irsyam et al., 2007)

2.3 Mohr-Coulomb Model

The mohr coulomb model is a soil framework distinguished by perfectly elastic and plastic characteristics. A perfectly plastic model is constitutive with a specific yield plane, fully defined by the model parameters and unaffected by deformation (plastic condition). The stress conditions represented by the points below the yield plane are characterized by elastic behavior, and the strain tends to return to its original state. Meanwhile, the points above the yield plane exhibit plastic behavior and the strain cannot return to its original state.

Furthermore, five parameters are needed for analysis using the mohr coulomb model, namely Young's modulus (E), Poisson's ratio (ν), internal friction angle (ϕ), cohesion (c), and dilatancy angle (ψ) (Brinkgreve et al., 2007). This study adopted the Undrained A method, where all parameters are in effective conditions. Table 2 shows the detailed effective parameters obtained from laboratory tests, including strength and stiffness. These were verified using the Plaxis Soil Test tool by trial and error until the best fitting stress-strain curve between the real triaxial curve and results from modeling were obtained. The details of this fitting curve are shown in Figure 4. Stiffness realized from the Triaxial CU is in undrained condition (E_u), although it was further converted to an effective state using the following equation.

$$E' = E_u \times 2 \times \left(\frac{1+\nu'}{3}\right) \quad (1)$$

Table 1. Soil parameter for mohr coulomb model

Location Sample	c' [kN/m^2]	ϕ' [^{0}]	ψ' [^{0}]	E_{50}^{ref} [kN/m^2]	ν
Deltamas	20	24	0	12000	0,3
Deltamas *peak*	77	24	0	125000	0,3
Karawang	28	23	0	15000	0,3
Walini Tunnel	80	30	0	130000	0,3
Slope 52	30	20	0	13850	0,3
Slope 67	75	14	0	15000	0,3

2.4 Hardening Soil Model

The hardening model has an unstable yield area which can expand when stretched. There are two types, namely, shear and compression hardening. Shear hardening is used to model strains that cannot return to their original state due to deviator stresses. Compression hardening is used to model the irreversible plastic strain caused by primary compression under unidirectional and isotropic loading. The isotropic hardens when using the special data from the drained triaxial test, with the stress-strain relationship approximated by a hyperbola as shown in Fig 2.

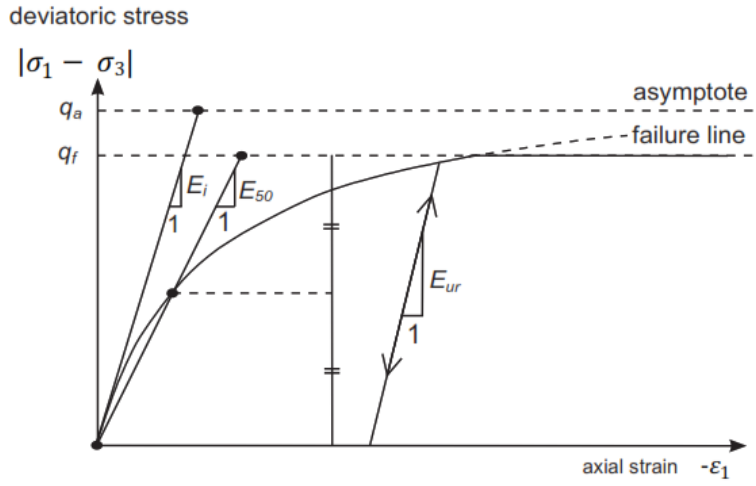

Figure 2. Hyperbolic stress-strain relationship (Brinkgreve et al., 2007)

The main HS parameters are generally similar to the MC model, namely Poisson's ratio (ν), internal friction angle (ϕ), cohesion (c), and dilatancy (ψ). Meanwhile, it has 3 types of stiffness, namely secant stiffness (E_{50}), tangent stiffness for primary oedometer loading (E_{oed}), and unloading reloading stiffness (E_{ur}). The Plaxis use of superscript notation "ref" that refers to the normalized pressure (P_{ref}) is 100 kPa. The last HS parameter is dependent on stress (m).

E_{50} and E_{ur} are obtained from a hyperbolic stress-strain relationship determined by the triaxial test result. Meanwhile, E_{50}^{ref} and m parameters are obtained from the cartesian plot using a logarithmic scale with normalized E_{50} by P_{ref} (E_{50}/p_{ref}) and confining stress (σ_3'/p_{ref}) in the y-axis and x-axis, respectively (Surarak, et al., 2012). Figure 3 shows how these are obtained.

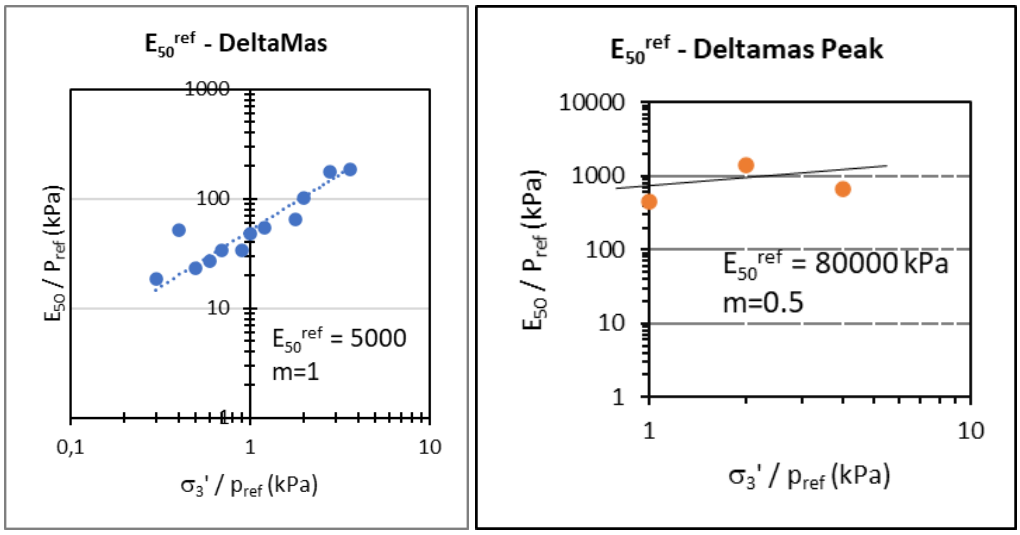

Figure 3. Logarithmic plot to determine E_{50}^{ref} and m parameter

The intersection between the trendline and y-axis in scale 1 shows the value of $E_{50}^{ref,}$ and the gradient indicates that of the m parameter. The detailed soil parameters for HS are shown in Table 3. E_{oed} and E_{ur} are obtained using the following equation.

$$E'_{ur} = 3 \times E'_{50} \quad (2)$$

$$E'_{oed} = k_{50} \times E'_{50}\text{, where } k_{50} \text{ equal to } 0{,}8 \quad (3)$$

Table 2. Soil parameter for hardening soil model

Location Sample	c' [kN/m²]	ϕ' [⁰]	ψ' [⁰]	E_{50}^{ref} [kN/m²]	E_{oed}^{ref} [kN/m²]	E_{ur}^{ref} [kN/m²]	Rf	m	K_0^{nc}	v_{ur}
Deltamas	20	24	0	4,500	8,200	13,500	0.9	1	0.5	0.3
Deltamas peak	77	24	0	70,000	125,000	210,000	0.9	0.5	0.57	0.3
Karawang	28	23	0	6,000	9,000	20,000	0.9	0.65	0.53	0.3
Walini Tunnel	80	30	0	60,000	60,000	180,000	0.9	0.5	0.43	0.3
Slope 52	30	20	0	6,000	9,000	18,000	0.9	0.5	0.6	0.3
Slope 67	75	14	0	9,000	16,000	27,000	0.9	0.65	0.66	0.3

The parameter and model verification outcome shown in Figure 4 indicates that the Deltamas data produces a relatively good fit curve and coincides with MC, HS, and the laboratory CU Triaxial results.

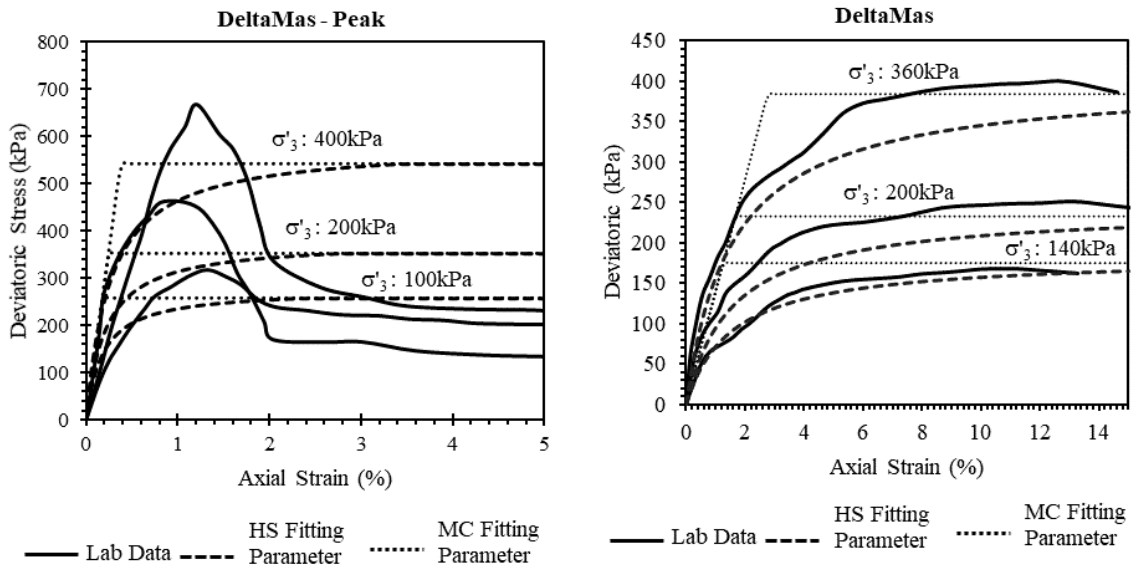

Figure 4. Best fitting curve to determine soil parameter using plaxis soil test tools

Meanwhile, the Deltamas Peak data shows that there is a large gap between the model and the Triaxial curve. It also forms a stress-strain curve that increases until it reaches its peak. It gradually decreases until a stationary condition where this level is known as the residual parameter is obtained. The shape of the curve shows that the clay shale characteristics of this location are reasonably fresh or unweathered. On the other hand, the data from Deltamas stated that it was quite weathered because the stress-strain graph only reached its peak and yield. Statistically, the MC and HS models are unsuitable for describing the behavior of unweathered clay shale soils, which possess both hardening and softening characteristics and a stationary graphic form. However, it is reasonably used to capture the deformation due to the construction process.

2.5 Parameter of Lining and Support System

The NATM tunnel and its support system, which includes rock bolt, forepolling, primary and secondary linings, were analyzed in this research. The primary lining is a composite material consisting of a steel profile grid with shotcrete C30 concrete modeled as a plate.

Table 3. Plate parameter for primary lining

Parameter	Unit	Value
EA	kN/m	11,744,318
EI	kN/m^2/m	119,890
d	m	0.35
w	kN/m/m	5.3
ν	-	0.2

Table 4 shows the required input parameters for the plate, namely EA, EI, w, d, and ν. In addition, E is the young modulus, A is the area or plate section, I is the inertia moment, d is the thickness, w is the weight, and ν is the Poisson's ratio. The values of E and w were calculated using the concept of weighted average between steel profile and shotcrete concrete. The model weight took into account the mass of soil lost by using the following equation.

$$w_{model} = \left(\gamma_{composite} - 0.5\gamma_{soil}\right) \times d_{real} \quad (4)$$

Secondary lining, forepolling, and inverted concrete are modeled as clusters with MC parameters (Ardiaca, 2009; Sivakugan et al., 2014) (Table 6), and the rock bolt is modeled as an embedded pile (Table 5).

Table 4. Embedded pile parameter for rock bolt

Type	$E_{composite}$ (kPa)	$\gamma_{composite}$ (kN/m^3)	T_{skin} (kPa)
D22	42,279,844	29.6	8.81
D42	97,397,923	46.2	11.66

Table 5. Mohr-Coulomb model parameter for concrete and forepolling composite

Parameter	Unit	Secondary lining (fc35)	Inverted Concrete (fc30)	Forepolling
Model	-	MC	MC	MC
Analysis type	-	Nonporous	Nonporous	Nonporous
UnSaturated Unit Weight (γ_{unsat})	kN/m^3	24	24	23
Saturated Unit Weight (γ_{sat})	kN/m^3	24	24	23
Horizontal permeability (kx)	m/day	-	-	-
Vertical Permeability (ky)	m/day	-	-	-
Undrained Elastic Modulus (Eu)	kN/m^2	27,805,575	25,742,960	920,000
Poisson's ratio (ν)	-	0,2	0,2	0,2
Undrained cohesion (c_u)	kPa	642	579	400
Undrained friction angle (ϕ_u)	^{0}	35	35	30
Tensile Cut-off	kPa	1050	900	-

The secondary lining uses a cluster model because it is impossible for plaxis to create a two-plate model that coincides with the primary lining. Meanwhile, to determine the magnitude of the force in the secondary lining, a plate-like structure is installed in the middle of its cluster with relatively small parameters to avoid causing a significant effect. The parameters for forepolling cluster employ the equivalence approach of the constituent composite materials, including forepolling, grouting material, and clay shale.

2.6 Analysis Using Plaxis

A tunnel's two-dimensional (2D) analysis requires some model adjustments to accommodate the arching effect in the 3-dimensional (3D) investigation. This is commonly realized using three approaches (Swoboda, 1990): the stiffness reduction method, load reduction method (Convergence-Confinement Method / CCM), and the modified stiffness reduction method. According to the Plaxis reference manual, the technique applied in this software is 60% of the CCM method, also known as deconfinement or β method.

The analysis is performed using the Undrained A method to get the best result because this approach is used to determine the stress by using effective parameters. Therefore, it predicts the pore pressure followed by a consolidation analysis under long-term conditions. (Brinkgreve et al., 2007)

Stage construction analysis in Plaxis 2D, as shown in Figure 5, includes (1) Initial conditions of analysis in K0-Procedure, (2) upper bench excavation with 60% deconfinement in 3 days, (3) activation of the primary plate lining and upper rock bolt, (4) excavation of the left and right sides of the middle bench with 60% deconfinement in 2 days, (5) activation of primary plate lining and rock bolt in the middle area, (6) excavation of the center side of the middle bench with deconfinement 60% in 1 day, (7) excavation of the left and right sides of the lower bench with deconfinement 60% in 1 day, (8) activation of the primary plate lining and rock bolt on the left and right sides of the lower bench, (9) excavation of the middle side of the lower bench with deconfinement 60% in 1 day, (10) activation of the primary plate lining on the bottom side, (11) activation of cluster secondary lining and plate (thin wall) in 1 day, (12) activation of inverted concrete in 1 day.

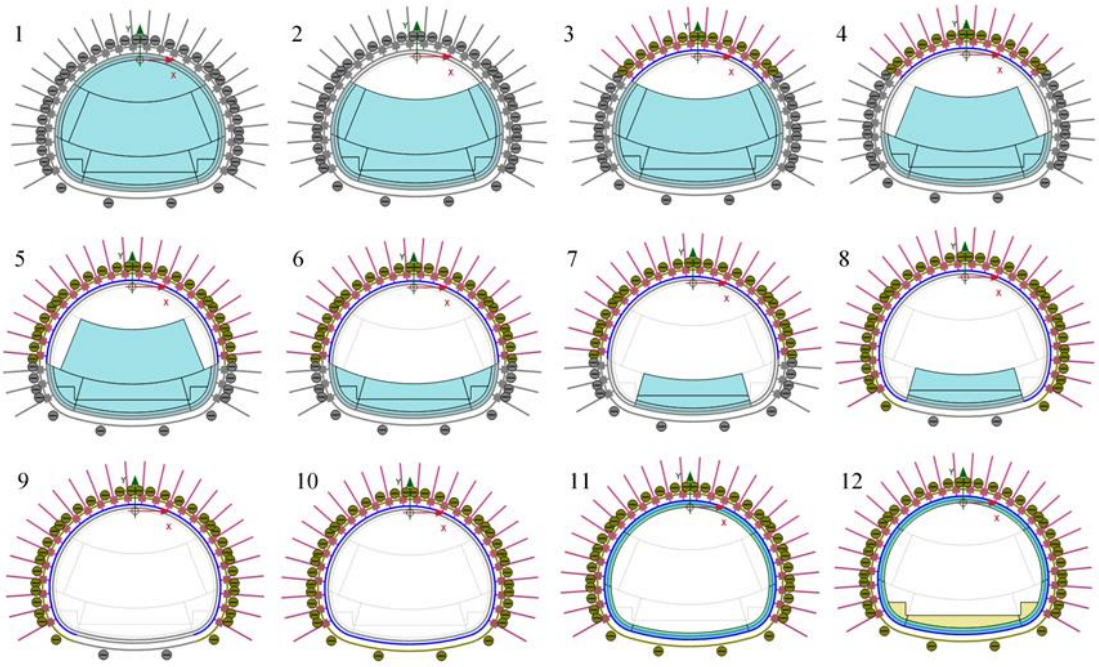

Figure 5. Stage construction analysis in plaxis 2-dimension

Analysis with Plaxis 3D is almost similar to 2D, where an example is shown in Figure 6. The 3D model eliminates the deconfinement stage and moves the construction stage forward by using the bench. (1) Initial conditions of analysis in K0-Procedure, (2) upper bench excavation for 1st segment in 3 days, (3) activation of the primary plate lining and upper rock bolt for 1st segment, (4) upper bench excavation for 2nd segment in 3 days, (5) activation of the primary plate lining and upper rock bolt for 2nd segment, (6) middle bench excavation for 1st segment in 3 days, (7) activation of the middle primary plate lining and rock bolt for 1st segment, (8) upper bench excavation for 3rd segment in 3 days, (9) activation of the primary plate lining and upper rock bolt for 3rd segment, (10) middle bench excavation for 2nd segment in 3 days, (11) activation of the middle primary plate lining and rock bolt for 2nd segment, (12) bottom bench excavation for 1st segment in 2 days, (13) activation of the bottom primary plate lining and rock bolt for 1st segment, (14) middle bench excavation for 3rd segment in 3 days, (15) activation of the middle primary plate lining and rock bolt for 3rd segment, (16) bottom bench excavation for 2nd segment in 2 days, (17) activation of the bottom primary plate lining and rock bolt for 2nd segment, (18) bottom bench excavation for 3rd segment in 2 days, (19) activation of the bottom primary plate lining and rock bolt for 3rd segment, (20) activation of cluster secondary lining and plate (thin wall) in 1 day, (21) activation of inverted concrete in 1 day.

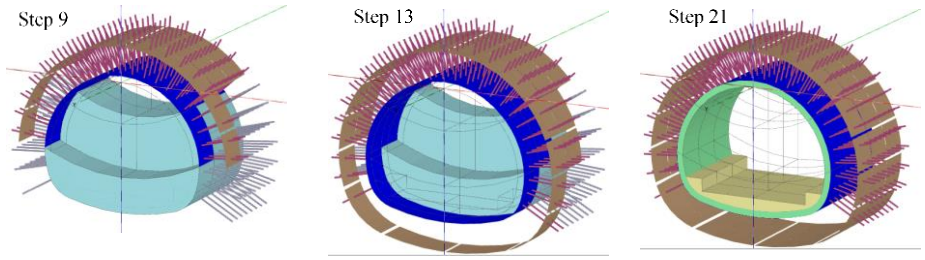

Figure 6. Examples of stage construction in plaxis 3-dimension

3 RESULT AND DISCUSSION

First, all parameters were compared by applying them to the model with geometry overburden 3-time tunnel diameter (3d) in the Plaxis 2D. The hardening soil model was selected to get a better result of stress and deformation. Parameters from Deltamas, Karawang, DK52, and DK67 produce

large deformation, more than 1 m; therefore, it is evident that these caused the tunnel's collapse. Meanwhile, the Walini tunnel and Deltamas peak data produced a deformation of 8.5 cm and 9 cm, respectively. With the model's limitations using 3d overburden and tunnel support as previously described, the correlations between cohesion, internal friction angle, and stiffness modulus were carried out to obtain an estimated parameter that meets the allowable deformation of 30cm. Table 7 shows that the parameter used for correlation and the calculation of effective shear strength (τ) was obtained using this equation $\tau = c + \sigma_v.\tan\phi$. The deformation value is the distortion that occurred in the crown of the tunnel, which was obtained from the plaxis modeling result. From the graphic equation in Figure 7, it is obvious that the minimum parameters needed to meet the 30 cm allowable deformation include shear strength (τ') 465 kPa, internal friction (ϕ') 28^0, cohesion (c') 53 kPa, $E'_{50}{}^{ref}$ 30,000 kPa, and $E'_{ur}{}^{ref}$ 90,000 kPa.

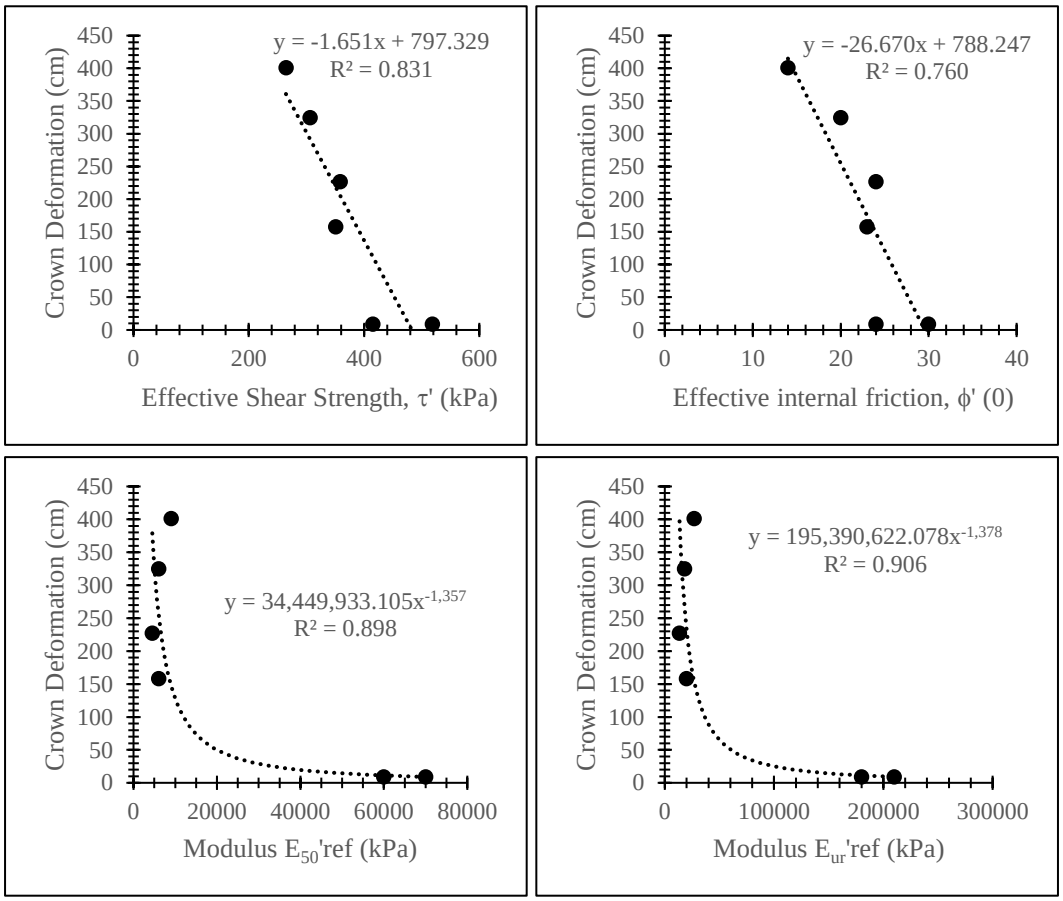

Figure 7. Correlation chart of shear strength parameters based on deformation in the crown

Table 6. Data and calculation for shear strength parameter correlation

Location of Soil Data	c' (kPa)	ϕ' 0	$E'_{50}{}^{ref}$ (kPa)	$E'_{ur}{}^{ref}$ (kPa)	Shear strength (kPa)	Deformation (cm)
Deltamas	20	24	4,500	13,500	358.4	227
Karawang	28	23	6,000	20,000	350.6	158
DK52	30	20	6,000	18,000	306.6	325
DK67	75	14	9,000	27,000	264.5	401
Deltamaspeak	77	24	70,000	210,000	415.4	9
Walini	80	30	60,000	180,000	518.8	9

Note: Calculation Shear strength using σ_v= 20 kN/m^3 x 38m = 760 kPa, where $\tau = c + \sigma_v.\tan\phi$

3.1 Comparison of MC and HS Soil Model

Comparison between MC and HS using the model with 3d overburden produces smaller crown deformation, but the differences are insignificant. This shows that the input parameters for the MC

and HS models gave a good response as modeled during its verification stage, where both produced similar deformation.

Figure 8 shows that the surface deformation of Walini and Deltamas data with MC models produces smaller deformations at the center of the tunnel; however, the effect is longer in the HS models. At a position 50 m from the tunnel center, the deformation of the HS model is approximately zero.

Figure 9 shows the shading pattern of deformation, vertical effective stress, and excess pore water pressure. The MC model produces greater effective stress both at the bottom and top of the tunnel (vertical effective stress) than the HS. Meanwhile, the MC produces lesser stress on the side (horizontal effective stress) than the HS model. The excess pore water pressure review shows that the MC model produces a positive (+) value at the top and bottom of the tunnel, greater than the HS. The difference at the top of the tunnel is quite large, while it is relatively the same size at the bottom. On the side, a negative excess pore water pressure (-) was produced with the MC model being greater than the HS.

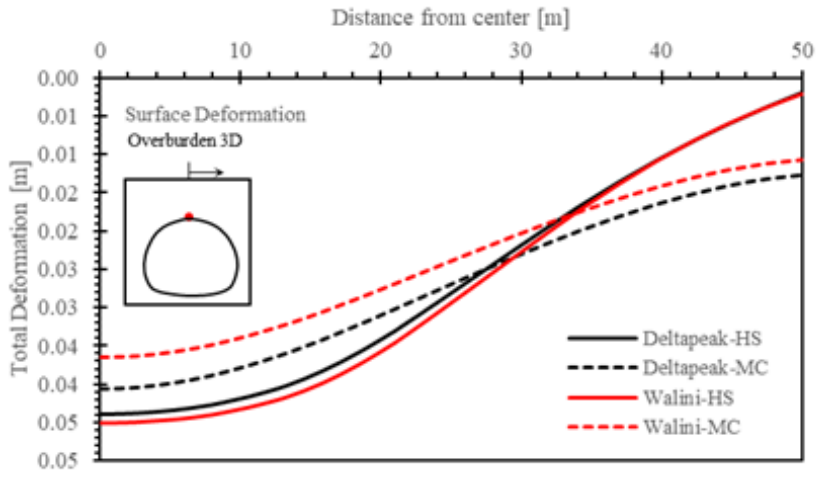

Figure 8. Surface deformation for the model with overburden 3d

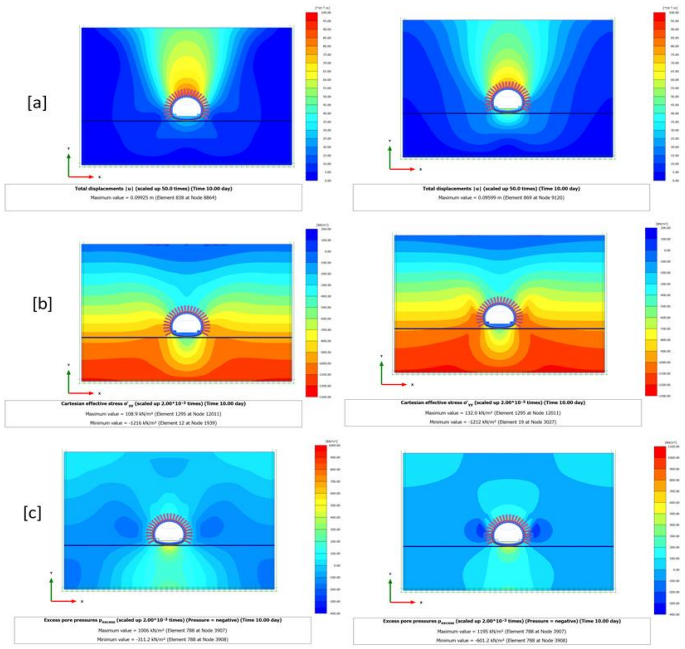

Figure 9. Comparison of shading contour of HS (left) & MC (right) in (a) total deformation, (b) vertical effective stress, (c) excess pore water pressure

3.2 Comparison of Short-Term and Long-Term Analysis

In the short-term condition, the arch-shaped deformation is concentrated on the upper side of the tunnel. In contrast, it spread throughout the model zone in the long-term condition due to excess pore water pressure dissipation (Figure 10).

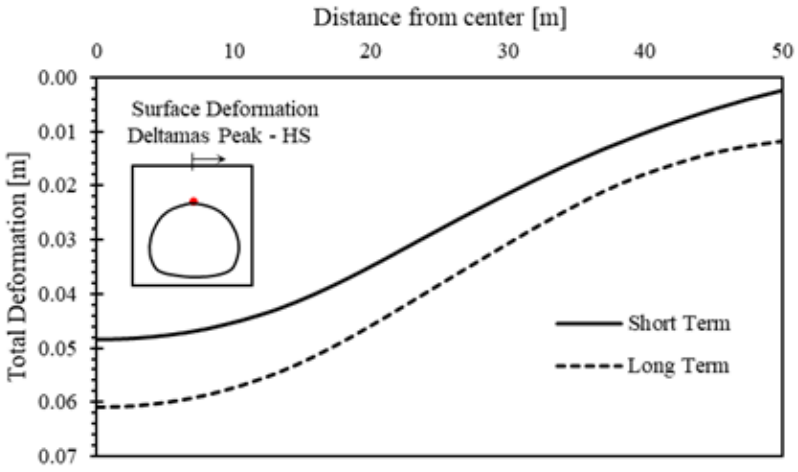

Figure 10. Surface deformation for the model with overburden 3d in short and long-term analysis

Long-term deformations increased after construction and increased tunnel lining stress, which needs to be considered during its design (Figure 11). The effective vertical stress both at the top and bottom of the tunnel has decreased from short to long term.

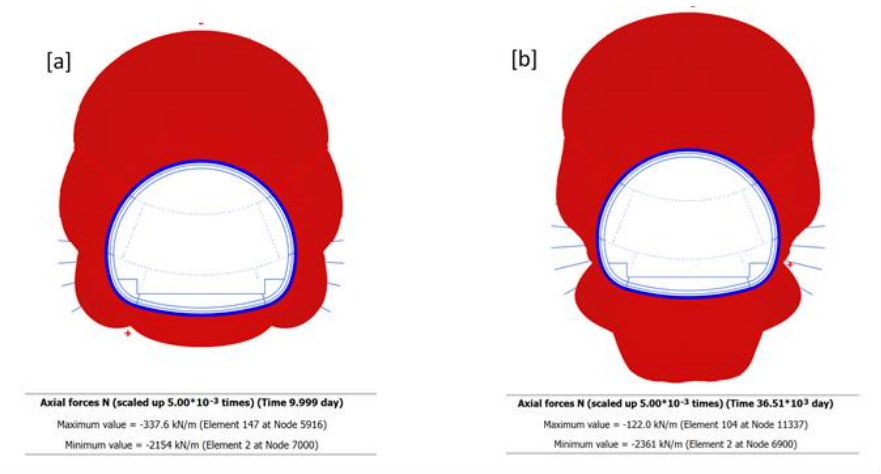

Figure 11. Axial force on tunnel lining for (a) short-term and (b) long-term

Meanwhile, the effective horizontal stress on the left and right sides of the tunnel recorded a slight increase under short and long-term conditions. The amount of excess pore water pressure formed is in line with the development of effective stress. The deformation at the top of the tunnel (crown) increases slightly in the short and long-term conditions. Reviewing the safety factor (SF) value shows that the long-term stability is lesser for both MC and HS models.

3.3 Comparison of Overburden Variations

Comparative analysis between 3D, 6D, and 9D overburden was carried out on Deltamas peak data using the Hardening Soil (HS) model. Observations of the total shading deformation show that the greater the overburden, the lesser or disappearance of the arching effect from the surface. Meanwhile,

the difference in surface deformation shows that the 6D and 9D models have relatively uniform graphs for the entire distance from the center tunnel with an equally slight decrease.

Observation of the crown of the tunnel (crown) shows that the greater the overburden, the greater the deformation, as shown in Figure 12. Moreover, in the long-term condition, the deformation of the three models is relatively uniform, and there is no significant addition. Meanwhile, when the distribution of the effective principal stress was studied, it was discovered that an arc-like type was formed at the end of the construction. Its magnitude decreases in long-term conditions, especially at the top and bottom of the tunnel. Furthermore, it is obvious that the greater the overburden, the greater the effective vertical stress at the initial conditions and the same elevation. However, a significant decrease was detected in the effective vertical stress at the end of construction (short term).

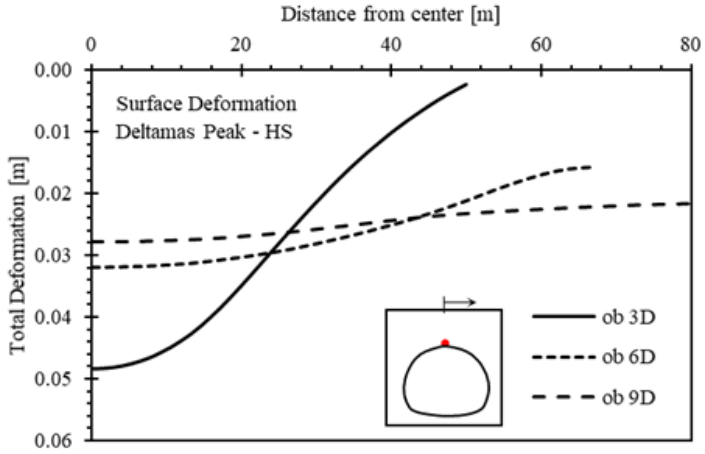

Figure 12. Surface deformation for the model with variation overburden

3.4 Comparison of 2D vs. 3D Analysis

Three-Dimensional (3D) model analysis was performed on Deltamas peak parameters using 3d overburden. The comparison of the deformation with the 2D model (Figure 13) shows the difference in the shading distribution. The deformation of the 3D model at the crown of the tunnel is 5.3 cm or equivalent to 50% smaller than the 2D model. This large gap is mostly caused by the assumption that 60 % of the deconfinement value at the deactivated soil cluster stage is unsuitable.

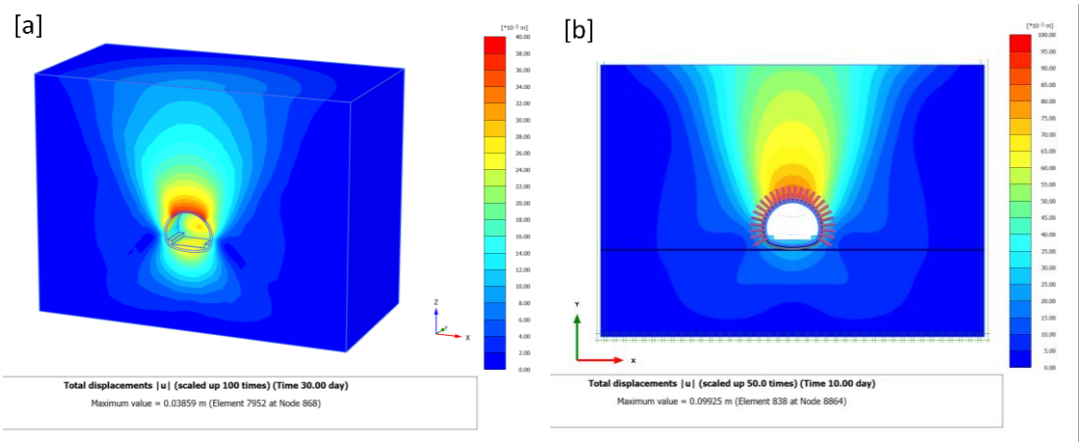

Figure 13. Shading total displacement between (a) Plaxis 3D and (b) Plaxis 2D

4 CONCLUSION

Clay shale in West Java is widespread over four rock formations, namely Cihoe (Tpc), Subang (Tms), Cantayan (Mtts/Mttc), and Jatiluhur (Tmj). Each of them has quite different mechanical and engineering properties. Stability analysis of tunnel on clay shale involves relatively complex geometry, construction sequence, excess pore-water pressure, and long-term behavior of the clay shale under tunneling process stress-path. The minimum effective parameters needed to support it during construction to meet the allowable deformation for 3d overburden conditions and the particular reinforcement system are c' 53kPa, ϕ' 28°, and $E'_{50}{}^{ref}$ 30,000 kPa. Further strengthening of the tunneling support systems in clay shale is required to meet the deformation criteria. The hardening soil model is more appropriate in terms of analyzing tunnel stability. The application of 2D tunnel modeling needs to be carefully analyzed, thereby representing the behavior of a continuous or 3D tunnel structure. Long-term deformations increase after construction and increase tunnel lining stress that must be considered in its design.

DISCLAIMER

The authors declare no conflict of interest.

AVAILABILITY OF DATA AND MATERIALS

All data are available from the author.

ACKNOWLEDGMENTS

The authors are grateful to PT WSP and CARS-DARDELA JO (CDJO) for providing data on clay shale soil in West Java. The authors are also grateful to Andhika Sahadewa, Ph.D., Eyrton Silaban, and engineers from CDJO for their support and in-depth discussion about the NATM tunnel construction process.

REFERENCES

Achdan, A. & Sudana, D., 1992. Peta Geologi Lembar Karawang, Jawa. Bandung: Pusat Penelitian dan Pengembangan Geologi.

Ameratungga, J., Sivakugan, N. & Das, B. M., 2016. *Correlation of Soil and Rock Properties in Geotechnical Engineering.* India: Springer.

Ardiaca, D., 2009. Mohr-Coulomb Parameters for modelling of concrete structur. *Plaxis Bulletin - Spring issue*, pp. 12-15.

Bobet, A. & Einstein, H. H., 2008. Deep Tunnels in Clay Shale: Evaluation of Key Properties for Short and Long Term Support. *Characterization, Monitoring, and Modeling of Geosystems*, pp. 406-467). Geocongress.

Bonini, M., Debernardi, D., Barla, M. & Barla, G., 2009. The Mechanical of Clayshale and Implication on the Design of Tunnels. *Rock Mechanics and Rock Engineering*, 361-388. doi:10.1007/s00603-007-0147-6

Bowles, J., 1996. *Foundation Analysis and Design fifth edition.* Singapore: McGraw Hill.

Brinkgreve, R., et al., 2007. *Plaxis 2D Versi 8 - Manual Model Material.* Belanda: Delft University of Technology & Plaxis b.v.

Deen, R. C., 1981. The need for Schema for the Classification of Transitional (Shale) Materials. *ASTM Geotechnical Testing Jurnal*, 4, pp. 3-10.

Effendi, A. C., Kusnama, & Hermanto, B., 1998. Peta Geologi Lembar Bogor, Jawa. *Edisi Kedua*. Bandung: Pusat Penelitian dan Pengembangan Geologi.

Gartung, E., 1986. Excavation in hard clays of a Keuper Formation. *Proceeding of Symposium, Geotechnical Engineering Division.* Seattle, Washington.

Irsyam, M., Susila, E. & Himawan, A., 2007. Slope Failure of an Embankment on Clay Shale at Km 97+500 of the Cipularang Toll Road and the Selected Solution. *International Symposium on Geotechnical Engineering, Ground Improvement and Geosynthetics for Human Security and Environmental Preservation*, (pp. 531 - 540). Bangkok.

Look, B. G., 2007. *Handbook of Geotechnical Investigation and Design Tables.* London: Taylor & Francis Group.

Sivakugan, N., Das, B., Lovisa, J. & Patra, C., 2014. Determination of c and phi of rock from indirect tensile strength and uniaxial compression tests. *International Journal of Geotechnical Engineering*, pp. 59-65.

Sudjatmiko, 1972. *Peta Geologi Lembar Cianjur, Jawa.* Bandung: Pusat Penelitian dan Pengembangan Geologi.

Surarak, C., Likitlersuang, S., Wanatowski, D., Balasubramaniam, A., Oh, E. & Guan, H., 2012. Stiffness and strength parameters for hardening soil model of soft and stiff Bangkok clays. *Soils and Foundations*, pp. 682-697. doi:http://dx.doi.org/10.1016/j.sandf.2012.07.009

Swoboda, G., 1990. Numerical Modelling of Tunnels. In C. Desai, & G. Gioda, *Numerical Method and Constitutive Modelling in Geomechanics* (pp. 277-318). Udine: Springer.

Terzaghi, K., Peck, R. & Mesri, G., 1996. *Soil Mechanics in Engineering Practice, 3rd Edition.* Canada: John Wiley & Sons.

Zarkasi, I., Irpani, H. & Arifien, H., 2018. Penanganan Jembatan Cisomang Ruas TOL Cikampek-Padalarang: Pembelajara Penanganan Jembatan Akibat Pergerakan Tanah Clayshale. *Jurnal HPJI*, 4(1), pp. 25-36.